

Pyrazole Bioisosteres of Leflunomide as B-Cell Immunosuppressants for Xenotransplantation and Chronic Rejection: Scope and Limitations

Christos Papageorgiou,*[†] Rainer Albert,[†] Philipp Floersheim,[‡] Michel Lemaire,[§] Francis Bitch,^{||} Hans-Peter Weber,[⊥] Elsebeth Andersen,[†] Valerie Hungerford,[†] and Max H. Schreier[†]

NOVARTIS Pharma AG, BAS-350.314, CH-4002 Basel, Switzerland, and Nova Research Services, CH-4143 Dornach, Switzerland

Received April 21, 1998

T-cell immunosuppressant-based therapies efficiently control early graft rejection in allotransplantation settings. They fail, however, to prevent those rejection events which are mediated by transplant-induced antibody (Ab) responses such as those involved in xenograft and chronic allograft rejection. This is mainly due to their inability to block T-cell-independent Ab production against the transplanted organs. The bioactive metabolite **2(Z)** of leflunomide (**1**) inhibits the formation of such Ab, but the drug has pharmacokinetic properties and a therapeutic window incompatible with transplantation indications. Pyrazole **3**, a constrained analogue of **2(Z)**, was designed and shown to be conformationally and biologically similar to **2(Z)**. Further investigations with derivatives of **3** demonstrated that the pyrazoles had very tight structure–activity relationships, the only equipotent compound being **3o**. However, in contrast to **2(Z)**, both **3** and **3o** were inactive in vivo due to short half-life and drug concentrations lower than the in vitro obtained IC₅₀ values. Compound **3o** inhibits T-cell-independent Ab production by a different biochemical mechanism from that of **2(Z)** and **3** and may therefore represent a valuable tool for the identification of new targets for B-cell inhibition.

Introduction

In contrast to allotransplantation where current immunosuppressive therapies overcome the effects of T-cell-mediated graft rejection¹ and antibody (Ab) formation against the graft,² antibody-mediated rejection is the first major obstacle toward clinical solid organ xenotransplantation,³ the transplantation of organs between individuals of different species. Indeed, xenogeneic immune responses mediated by preexisting, naturally occurring antibodies and complement lead to hyperacute and acute rejection of vascularized organ grafts. These issues have been investigated in the pig to non-human primate model of heart xenotransplantation, where the presence of monkey xenoreactive natural antibodies to pig antigens and their attachment to the vascular endothelium of pig organs stimulated the classical pathway of complement activation and led to the irreversible loss of the heart because of hyperacute rejection.⁴ On the basis of genetic engineering, significant progress has been made to avert hyperacute rejection as demonstrated in monkey transplantation studies with pig transgenic hearts expressing human decay accelerating factor (DAF), a species-specific inhibitor of complement activation.⁵ However, if complement activation is blocked in the absence of immunosuppression and the xenografts survive hyperacute rejection, the graft is still lost due to acute vascular rejection since excessive Ab production is induced by the

transplanted xenograft.⁶ Therefore, Ab production by B cells is a key event both during the hyperacute rejection phase and during the acute rejection phase of xenotransplantation. No participation of T cells is required for these phenomena to occur, as demonstrated by the failure of T-cell immunosuppressants such as cyclosporin in xenotransplantation and the rejection of hamster heart xenografts by T-cell-deficient nu/nu rats.⁷

A second syndrome associated with the presence of Ab is chronic rejection (graft vessel disease, late graft rejection), a disease leading to organ loss due to the obstruction of arterial vessels of the transplanted allograft. Persistent endothelial injury leads to intima proliferation, smooth muscle cell migration, and matrix deposition as key features of this complex process which proceeds over many years after transplantation.⁸ Among the large number of contributing factors leading to endothelial cell damage, Ab and complement are the most critical components. Evidence that humoral activity is responsible for graft vessel disease includes, among others, the presence of anti-HLA Ab in rejecting patients' sera and the vascular deposition of complement-fixing immunoglobulin in areas of intimal thickening.⁹ The importance of B cells in graft vessel disease has also been demonstrated in in vivo models; only minimal neointima formation is seen in carotid arteries transplanted into B-cell-deficient mice.¹⁰

Drugs which inhibit Ab formation and are effective in xenotransplantation models can also be expected to alter the progression of chronic rejection. Confirmation has been obtained with leflunomide (**1**), a compound which interferes with T-cell and B-cell function through the selective inhibition of dihydroorotate dehydrogenase (DHODH), a rate-limiting step of the de novo pyrimidine biosynthetic pathway of cells.¹¹ Indeed, data obtained

* Corresponding author. Tel: 0041-61-3246188. Fax: 0041-61-3243036. E-mail: christos.papageorgiou@pharma.novartis.com.

[†] Transplantation Research, NOVARTIS.

[‡] Nervous System, NOVARTIS.

[§] Drug Safety, NOVARTIS.

^{||} Central Functions, NOVARTIS.

[⊥] Nova Research Services.

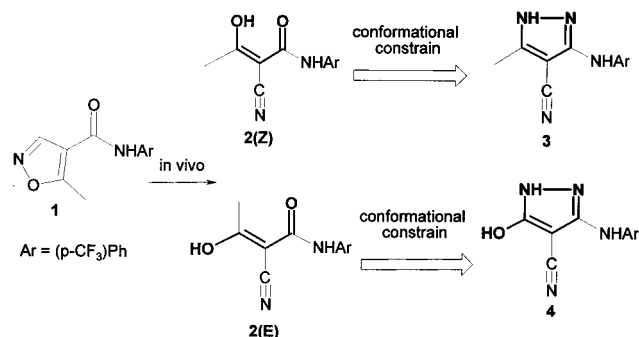


Figure 1. Structural relationships between leflunomide (**1**), its bioactive metabolite **2(Z)** or **2(E)**, and the corresponding pyrazoles **3** and **4**, respectively.

with leflunomide in animal models demonstrate that the drug can prevent Ab-mediated rejection in heart xenotransplantation¹² and that it can control the progression of chronic rejection.¹³

Leflunomide's potential for transplantation indications is clearly limited by its undesirable pharmacokinetics (mean $t_{1/2}$ in humans: 300 h)¹⁴ that do not allow easy adjustment of the immunosuppressive regime. Moreover, when **1** is given to rats in combination with the standard antirejection drug cyclosporin A (CsA), it has a very narrow therapeutic window. This is also the case for the published leflunomide analogues which have a shorter half-life in humans than leflunomide.^{15,16}

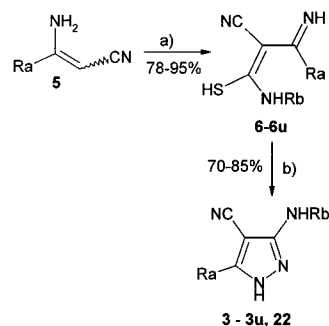
Design Concept

Searching for drugs which prevent Ab responses, we desired a lead compound with a pharmacological profile similar to that of leflunomide and shorter half-life. To this end, the bioactive metabolite of leflunomide was considered (Figure 1). Indeed, **1** is a prodrug whose isoxazole ring is quickly and quantitatively opened in vivo to give the bioactive hydroxycyanopropenamide **2**. Among the two possible geometric isomers, **2(Z)** and **2(E)**, the former having an enol structure stabilized by a strong hydrogen bond between the OH and the amide carbonyl was observed in the solid state by X-ray crystallographic analysis.¹⁷ Moreover, **2(Z)** is believed to be the bioactive isomer on the basis of physicochemical investigations of this compound class in solution¹⁸ and molecular modeling calculations.¹⁹ Consequently, two substituted pyrazoles (**3** and **4**) were designed as conformationally constrained analogues of the corresponding possible structures of leflunomide's bioactive metabolite, **2(Z)** and **2(E)**, respectively, and only one was expected to be biologically active (Figure 1). Care was taken in the design to not only keep the conjugated system unchanged but also keep the molecular volumes.

Synthesis

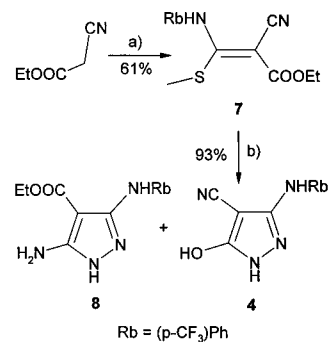
The synthesis of the required pyrazoles was based on the reaction of acidic methylene compounds with isothiocyanates followed by treatment of the resulting thioamides with hydrazine (Schemes 1 and 2).^{20,21} Starting from ethyl cyanoacetate, the pyrazole **4** was obtained together with the 4-ethoxycarbonyl-5-amino derivative **8** in a 20/80 ratio as a consequence of the two possible ring closures of the thiomethyl intermediate **7**.²² For compound **3** as well as for the preparation of the closely related analogues **3a–u**, the corresponding 3-amino-

Scheme 1^a



^a (a) RbNCS (1.0 equiv), dioxane, reflux, 3–6 h; (b) H₂NNH₂ (1.2 equiv), EtOH, reflux, 2–3 h.

Scheme 2^a

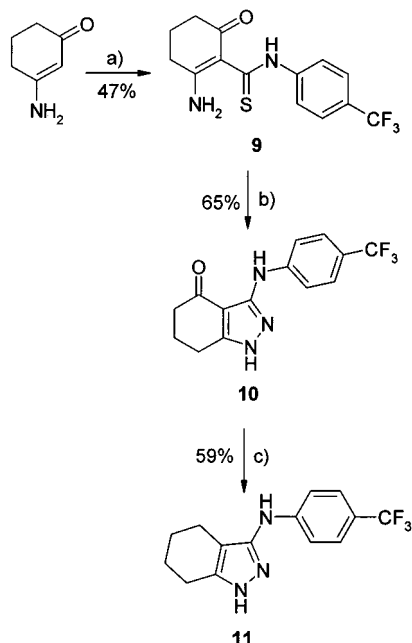


^a (a) (i) NaH (1.2 equiv), (ii) (p-CF₃)PhNCS (1.2 equiv) then MeI (1.2 equiv); (b) H₂NNH₂ (1.2 equiv), EtOH, reflux, 3 h.

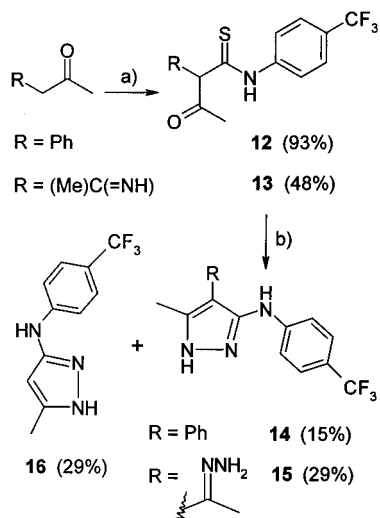
noacrylonitriles **5** were employed as starting materials which were obtained either via treatment of alkyl- β -ketoacetonitriles with NH₃ in a sealed vessel²³ or from the reaction of the sodium salt of acetonitrile with the appropriate aryl nitriles.²⁴

Additional pyrazole derivatives required for structure–activity investigations were synthesized according to Schemes 3–5. The tetrahydro-4*H*-indazolone **10** was obtained upon reaction of the commercially available 2-aminocyclohexenone with (p-CF₃)PhNCS followed by cyclocondensation of the resulting thioamide **9** with hydrazine.²⁵ The corresponding indazole derivative **11** was prepared through reduction of **10** with AlH₃, the intermediate allylic alcohol being too reactive to isolate. The influence of the 4-cyano substituent was probed via its replacement with a phenyl and ethoxycarbonyl electron-withdrawing groups as well as with hydrazino and alkyl moieties (Scheme 4). The 4-Ph-substituted pyrazole **14** was prepared via acylation of the sodium salt of benzyl methyl ketone with (p-CF₃)PhNCS and subsequent reaction with hydrazine.²⁶ The analogous reaction of the thioamide **13** furnished the 4-hydrazino compound **15** together with an equal amount of **16**, the des-CN derivative of **3**, whose formation is the consequence of the elimination of the acetyl moiety of **13**. No trace of the corresponding methyl ketone could be detected under a variety of experimental conditions.

The key reaction leading to **17** was the cyclocondensation of the commercially available (p-CF₃)phenylthiosemicarbazide with ethyl 2-chloroacetoacetate.²⁷ Subsequent reduction of the ester functionality under mild conditions led to the allylic alcohol **18**, while the use of LiAlH₄ yielded exclusively the corresponding 4-methylpyrazole **19** (Scheme 5). Both reactions proceeded in

Scheme 3^a

^a (a) (*p*-CF₃)PhNCS (1.1 equiv), MeCN, reflux, 18 h; (b) H₂NNH₂ (1.2 equiv), EtOH, reflux, 18 h; (c) LiAlH₄ (3.0 equiv), H₂SO₄ (1.5 equiv), THF, -78 °C to rt.

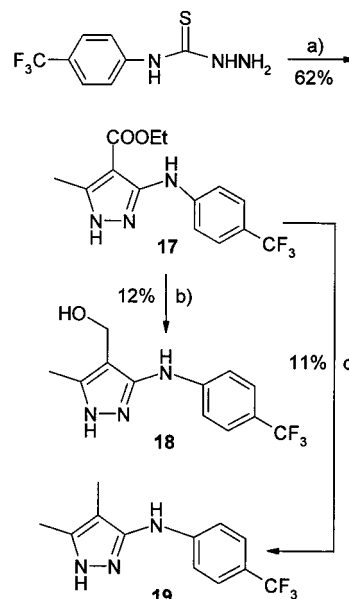
Scheme 4^a

^a (a) (i) (*p*-CF₃)PhNCS (1.2 equiv), THF, (ii) NaH (1.2 equiv); (b) H₂NNH₂ (1.3 equiv), EtOH, reflux, 18 h.

low yields and were accompanied by extensively decomposed starting material.

Structural Results

Among the two designed isomeric pyrazoles **3** and **4**, only **3** was biologically active (see biological results). Consequently and in order to check the structural similarity of **2(Z)** with **3**, the conformation of the latter in the solid state was investigated and compared with that of **2(Z)**.¹⁷ To this end, triclinic and monoclinic crystal forms were obtained from a MeOH/water solution which were initially thought to correspond to the two possible tautomeric forms of **3**. Subsequent X-ray analysis of each crystal form demonstrated that both corresponded to the same tautomer and that they adopted identical spatial arrangements. Indeed, **3** is

Scheme 5^a

^a (a) Concentrated HCl, 10 min then MeCOCH(Cl)COOEt (1.0 equiv); (b) LiAlH₄ (4.0 equiv), H₂SO₄ (2.0 equiv), THF, -78 °C to rt; (c) LiAlH₄, THF, reflux, 2 h.

characterized by the coplanarity of the pyrazole and phenyl rings and the *cis* arrangement of N(2)-C(3)-N(6)-C(7). For this highly compact structure to be formed, an unprotonated sp²-N(2) is required in order to avoid the interaction of the N(2) hydrogen with that of C(8). The driving force for the crystal packing observed is not due to the energetic contribution of a H-bond between the acidic H-C(8) and the imine N(2)²⁸ since the corresponding distance is 2.2 Å. If, alternatively, N(2)-C(3)-N(6)-C(7) were *trans*, the steric hindrance between the phenyl and the cyano group would again require loss of coplanarity. In conclusion, a planar structure of the pyrazole is energetically the most favorable one in the solid state, and it is only compatible with the tautomeric form of **3**. Clearly, the conformation observed for this molecule in the solid state does not provide any direct information on its conformational preferences in solution, but the presence of this folding pattern in the crystals suggests that a similar folded conformation is energetically accessible in solution too. Moreover, the recovery of the diffracting crystals out of a physiologically compatible solvent suggests that the experimentally determined conformation of **3** could indeed be identical with its bioactive one. Interestingly, ¹H NMR experiments conducted with **3** in DMSO-*d*₆ also indicate the presence of the same tautomer. Indeed, although a tautomeric exchange of the proton cannot be excluded, a NOE is observed between the methyl substituent and the H of N(1).

The structural similarity of the bioactive pyrazole **3** and **2(Z)** is shown in Figure 2. Clearly the pyrazole ring is a bioisosteric replacement for the hydroxycyanopropanamide moiety of leflunomide's metabolite, and the two molecules share similar conformations and molecular volumes (185.1 and 187.9 Å³ for **2(Z)** and **3**, respectively).²⁹ Despite the difference in ring size, a five ring versus a pseudo-six ring, the conjugated systems O-C=C-C=O in **2(Z)** and N-C=C-C=N in **3** superimpose with a RMS of 0.36 Å.

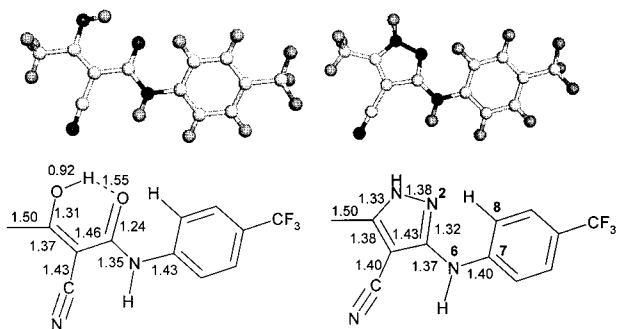


Figure 2. ORTEP plots and interatomic distances (Å) of hydroxycyanopropenamide **2(Z)** and pyrazole **3**.

Table 1. In Vitro Profiles of Reference and Designed Compounds

compd	type I ^{a,b}	MLR ^{a,c}	Jurkat ^{a,d}	DHODH ^{a,e}
CsA	>100	0.006	>10	>50
1	5.1	7.4	41.4	13
2(Z)	4.4	6.3	38.5	0.2
3	5.3	2.1	>50	2.6
4	>50	ND	ND	>50

^a IC₅₀ values in μM . Mean of at least three independent determinations. ^b Inhibition of the in vitro murine antibody response to T-cell-independent B-cell antigen TNP-LPS (type I). ^c Inhibition of the mouse mixed lymphocyte reaction. ^d Inhibition of Jurkat cell proliferation. ^e Inhibition of human dihydroorotate dehydrogenase. ND, not determined.

In Vitro Biological Results and Discussion. The activation of B cells can proceed by at least two fundamentally different mechanisms, one that requires B-cell contact with CD4⁺ T cells and one that is induced by antigen contact with B cells in the absence of CD4⁺ T cells. Two types of T-independent B-cell responses can be elicited depending on the antigen used. Type I responses are elicited by antigens such as TNP-LPS, whereas type II responses are elicited by antigens such as DNP-Ficoll. A murine assay for the evaluation of T-cell-independent B-cell responses was established, and it was found that leflunomide inhibits type I responses in vitro and in vivo while CsA does not (Table 1). Both compounds were inhibitors of the type II responses, with IC₅₀ of 5.5 μM and 4.0 nM, respectively. The failure of CsA, a T-cell immunosuppressant,³⁰ in animal models of xenotransplantation and the ineffectiveness of therapeutically relevant CsA doses to control the decline of long-functioning grafts in humans underline the importance of the T-cell-independent B-cell component and, in particular, the inhibition of the CsA-resistant type I responses. Consequently, this cellular assay was fundamental for the screening of the B-cell inhibitors required. In addition, the immunosuppressive activity of the compounds as well as their cytotoxicity was assessed in the mouse mixed lymphocyte reaction (MLR)³¹ and Jurkat proliferation assays, respectively, as an estimate of their therapeutic window. The biochemical mechanism of action of the compounds was compared to that of leflunomide using the human DHODH enzymatic assay.³²

The results of Table 1 demonstrate that, among the two designed pyrazoles, only compound **3** is immunosuppressive. Indeed, it inhibits both type I responses and the mixed lymphocyte reaction with IC₅₀ values comparable to those of leflunomide's metabolite **2(Z)**. In addition, the new compound has a better MLR/Jurkat

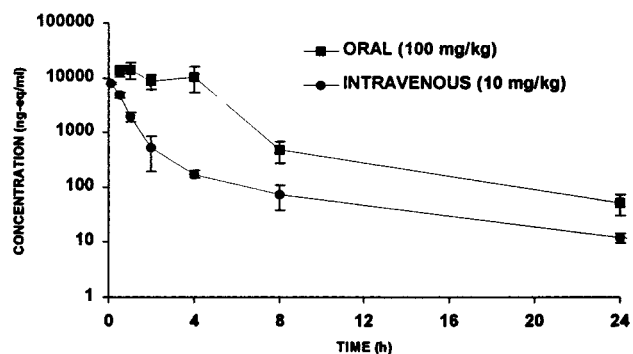
ratio than **2(Z)** indicating that it may have a lower general toxicity. These effects of **3** are at most partially mediated through DHODH inhibition since it has a 13-fold higher IC₅₀ than **2(Z)**. The lower affinity of the pyrazole and the associated $\Delta\Delta G = 1.56$ kcal/mol ($T = 298$ K) indicate the possible loss of a H-bond interaction with the enzyme.³³ The isomeric pyrazole **4** is devoid both of B-cell activity and of enzymatic activity up to high micromolar concentrations. Importantly, the ensemble of the biological data establishes unequivocally that the bioactive metabolite of leflunomide (**1**) has a Z-enol structure.

Having demonstrated that **3** behaves as an isostere of leflunomide's bioactive metabolite **2(Z)**, an extensive investigation of structure-activity relationships was undertaken with the hope that more active derivatives of **3** could be identified. Consequently, the influence of substitution at positions 1, 2, 4, and 5 of the pyrazole ring as well as that of variations of the aromatic moiety was studied, and the outcome is summarized in Table 2. Attempts to replace the anilinic nitrogen of **3** by carbon or oxygen were fruitless due to synthetic issues.

The data of Table 2a show that a para electron-withdrawing group on the aniline is necessary for B-cell inhibition in the low-micromolar range, while for enzyme inhibition a para hydrophobic group is required, the best being compound **3f** with an IC₅₀ = 0.5 μM . An analysis of the impact of the position of the aromatic substituent on the DHODH activity in the pyrazole and leflunomide series indicates that ortho and para substituents are detrimental for enzyme inhibition in both substance classes.^{15,17} Overall, pyrazole **3** has the best in vitro profile among the derivatives **3a-m** since it combines potent B-cell inhibitory activity and immunosuppression, as indicated by the MLR data, and shows no cytotoxic effects as assessed in the human transformed Jurkat cell line. The focus of further structure-activity work was the elucidation of the role of the 5-Me of **3** via its substitution by aromatic (**3u**), heteroaromatic (**3q-u**), amino (**3v,w**), and alkyl groups (**3n-p**). With the exception of the latter modifications, all the others were detrimental for both the enzyme and B-cell inhibition (Table 2b). Furthermore, among the alkyl derivatives, only **3p**, the 5-cyclopentyl one, is inactive. This result together with the results obtained with the aromatic derivatives **3q-u** indicates that steric bulk is not tolerated at position 5. However, the 5-iPr and 5-tBu derivatives **3n,o**, respectively, are equipotent to **3** concerning the B-cell inhibitory activity, and are not cytotoxic. Interestingly, in contrast to **3**, which mediates its effects through blockade of the DHODH activity, **3o** is not an enzyme inhibitor. In the hydroxypropenamide series, the analogous tBu derivative is a 70-fold weaker DHODH inhibitor (IC₅₀ = 16.2 μM) than the parent compound **2(Z)** and is devoid of type I activity up to 50 μM .¹⁷ This unexpected data indicates that inhibition of B-cell responses to the TNP-LPS antigen and overall immunosuppression can be achieved by a mechanism which operates independently of DHODH inhibition. Next, the influence of the 4-CN moiety of **3** was investigated by replacing it by a Ph and ester electron-withdrawing groups as well as by alkyl groups. The outcome of these studies indicates that **3** is by far

Table 2. Structure–Activity Relationships

compd	R	type I ^{a,b}	MLR ^{a,c}	Jurkat ^{a,d}	DHODH ^{a,e}
a. Influence of the 3-Aniline Substituent					
3	<i>p</i> -CF ₃	5.3	2.1	>50	2.6
3a	<i>m</i> -CF ₃	>50	ND	ND	>50
3b	<i>o</i> -CF ₃	>50	ND	ND	>50
3c	Ph	>50	>50	>50	>50
3d	<i>p</i> -F	9.2	7.4	>50	19.4
3e	<i>p</i> -CN	11.6	6	>50	3.2
3f	<i>p</i> -OCF ₃	20	0.45	16.1	0.5
3g	<i>p</i> -NO ₂	6.5	4.3	>50	9.0
3h	<i>p</i> -tBu	30.6	7.6	12.3	3.6
3i	<i>p</i> -Me	>50	ND	ND	12.1
3j	<i>p</i> -NH ₂	>50	ND	ND	>50
3k	<i>o,o',p</i> -tri-F	35	ND	ND	22.4
3l	<i>m,m'</i> -di-CF ₃	28.0	6.7	16.2	>50
3m	<i>p</i> -CF ₃ , <i>m</i> -Br	20.9	ND	ND	>50
b. Influence of the 5-Substituent					
3	Me	5.3	2.1	>50	2.6
3n	iPr	4.7	3.1	>50	4.0
3o	tBu	5.8	5.3	>50	>50
3p	cyclopentyl	22.4	2.9	31.8	>50
3q	3-pyridyl	27	ND	ND	>50
3r	4-pyridyl	13.6	3.6	10.8	>50
3s	2-thienyl	>50	ND	ND	>50
3t	2-furanyl	>50	ND	ND	>50
3u	Ph	32	ND	ND	>50
3v	H ₂ N	14.7	3.7	>50	>50
3w	EtNH	16.9	7.5	38.7	>50
c. Influence of the 4-Substituent					
3	CN	5.3	2.1	>50	2.6
14	Ph	29.4	ND	ND	>50
15	C(Me)NNH ₂	17.4	20.3	41.0	>50
16	H	26.5	16.5	>50	16.5
17	EtOOC	23.8	ND	ND	>50
18	Me	14.6	18.7	43.0	22.5
19	CH ₂ OH	21.3	ND	ND	2.7
d. Miscellaneous					
3		5.3	2.1	>50	2.6
10		16.7	8.6	17.7	6.5
11		13.8	3.4	31.2	6.2
20		19.1	23.6	>50	>50
21		23.1	16.1	47.2	>50
22		17.1	40.5	>50	>50

^{a–e}See corresponding footnotes in Table 1.**Figure 3.** Concentration of [³H]-**3** in blood after oral and intravenous administration. Results are mean ± SE of three mice.

the most potent compound (Table 2c). Methylation of the aniline N or of the N(2) of **3** or replacement of the (*p*-CF₃)aniline moiety by a (*p*-CF₃)benzylamino one resulted in total loss of the enzymatic activity and 3–5-fold reduction in the B-cell activity (Table 2d). In an attempt to include both an electron-withdrawing substituent and an alkyl substituent in a cyclic structure, the indazole **10** was obtained which represents one of the rare cytostatic compounds of the series. Taken together, the structure–activity relationships indicate that, in addition to compound **3**, only the corresponding 5-isopropyl and 5-*t*Bu derivatives **3n,o** fulfill the requirement set, that is, potent inhibition of the cyclosporin-resistant type I B-cell responses, potent immunosuppression, and lack of cytotoxicity.

In Vivo Evaluation/Pharmacokinetics. Among the three potent in vitro B-cell inhibitors (**3**, **3n,o**) discovered, a DHODH modulating compound and a compound acting independently of enzyme inhibition were chosen for further investigations. Consequently, **3** and **3o** were tested in vivo for inhibition of murine TNP-LPS responses after oral and subcutaneous administration of 100 and 50 mg/kg, respectively, and were found inactive as assessed by the lack of inhibition of TNP-specific immunoglobulin M (IgM) and G (IgG) titers. At this dose, leflunomide inhibited IgM and IgG by 61% and 97%, respectively. As expected, cyclosporin A was inactive in this model. To gain insight into possible reasons for the discrepancy between the in vitro and in vivo results obtained with the two pyrazoles, **3** was labeled with ³H at the meta position of the aniline via ³H₂ reduction of the corresponding bromo derivative and employed for pharmacokinetic studies. The radio-labeled compound was administered to male mice orally (100 mg/kg) or intravenously (10 mg/kg), and pharmacokinetic parameters were analyzed. Maximum blood concentrations of [³H]-**3** were achieved 0.5 h after oral application and persisted up to 4 h postdose (1–2.5 μM). The dose-normalized AUC ratio (po/iv) of radioactivity pointed out to a very good absorption (81%) of the pyrazole. The blood–concentration time profile (Figure 3) suggested a saturable presystemic first-pass and biphasic kinetics with a main half-life = 0.4 h. The compound was strongly bound to plasma proteins (fraction free ≈ 1.5%) but moderately distributed to tissues (*V*_{ss} = 1.4 L/kg). The total body clearance (CL) amounted to 1.0 mL/min after iv administration; the blood levels of total radioactivity were about double those of [³H]-**3** itself, pointing to an important metabolic clearance.

On the basis of the above results and hypothesizing that **3o** might be metabolically more stable than **3** due to the absence of the allylic methyl moiety and the presence of the tBu group which could shield the NH from enzyme-mediated conjugation, its plasma concentration as function of time was investigated. For this study 10 mg of **3o** was given orally to mice and the concentration of the compound was quantified by LC-MS/MS after 0.5, 1, 2, 4, and 8 h. The results obtained were similar to those seen with **3**. Indeed, **3o** had a short half-life ($t_{1/2} = 0.5$ h), and plasma concentrations in the 1 μ M range persisted for approximately 4 h. When comparing these data with those obtained after po administration of 100 mg/kg **3**, it appears that **3o** has a 10-fold increased stability as regards enzymatic degradation.

Conclusions

The structural and the in vitro biological results obtained with **3** emphasize its bioisosteric relationship with leflunomide's bioactive metabolite **2(Z)**. Indeed, both compounds inhibit T-cell-independent B-cell responses to the TNP-LPS antigen (type I), are immunosuppressive, and share a common biochemical target. Therefore, **3** fulfills the requirement for a B-cell inhibitor modulating cyclosporin A-resistant effects such as those involved in xenotransplantation and chronic rejection. Interestingly, the outcome of the structure-activity investigations with derivatives of **3** revealed that there is no correlation between inhibition of Ab formation and DHODH inhibition. Since enzyme inhibition is not a prerequisite for type I inhibition, the tBu derivative **3o** provides a valuable tool for the identification of new targets for B-cell intervention.

A 2-fold evidence is provided that the above conclusions are valid despite cellular data generated with murine systems and enzymatic data with human enzyme. First, the rat versus human sequence alignment of the enzymes indicates a 86.8% identity which indicates that no large discrepancies should be expected between human and the mouse enzyme which has not as yet been cloned. Second, and most important, competition mouse MLR experiments done with **3** and **3o** in the absence and presence of uridine showed that only the inhibitory activity of **3** could be affected by the nucleoside. Indeed, addition of 50 and 100 μ M of uridine in the MLR culture led to a reduction of the IC₅₀ of **3** by 30% and 44%, respectively, as compared to the control.

In contrast to leflunomide (**1**), the two most potent pyrazoles (**3** and **3o**) failed to inhibit murine IgM and IgG antibody responses in the TNP-LPS model in vivo after either oral or subcutaneous administration. The absorption and disposition studies carried out with radiolabeled **3** indicated that absorption was not a drawback and that high blood concentrations persisted for 4 h. Given the highest dose applied in the in vivo pharmacological studies (100 mg/kg, po), the extrapolation of the pharmacokinetic results indicates that approximately 1 μ M concentrations of **3** must have been obtained. These concentrations are 5-fold lower than the IC₅₀ values of the compound in B-cell inhibition (Table 1). Analogous results were obtained after exposure studies conducted with the metabolically more stable derivative **3o**. The pharmacokinetic studies offer

a plausible explanation for the failure of the compounds in vivo. Not only were drug levels less than the measured IC₅₀ values obtained, but they also persisted for a relatively short time period thus allowing the fast onset of antibodies against the TNP-LPS antigen.

In conclusion, despite the successful drug design approach and the in vitro efficacy of pyrazoles **3** and **3o**, the compounds fail to attain therapeutically relevant concentrations in vivo. The very tight structure-activity relationships with this compound class represent a severe limitation for the identification of further compounds with improved pharmacokinetic properties. Taken together, the results of this work illustrate the importance of the combination of drug design with absorption, distribution, and metabolic studies in order to ensure the quality of the compounds involved in drug discovery programs.

Experimental Section

(1) Chemistry. Compounds were characterized by 400-MHz proton NMR at room temperature using a Bruker MX-400 or DPX-400 spectrometer. Chemical shifts are expressed as ppm downfield from tetramethylsilane; J values are expressed in Hz. Fast atom bombardment mass spectroscopy (Xe, 8 keV) on a VG70-SE mass spectrometer was used for the characterization of all reported compounds. C, H, and N analyses were carried out with all substances biologically evaluated, and $\pm 0.4\%$ was acceptable. For chromatographic purifications, the flash chromatography technique was applied using 230-400 mesh silica gel.

2-Cyano-3-imino-N-(Rb)thiobutyramides 6-6u: General Procedure. 3-Iminoalkyl(aryl)onitrile (1 equiv) and the respective aromatic isothiocyanate (1 equiv) were dissolved in dioxane (~10 mmol in 40 mL) and refluxed for 3-6 h. After removal of the solvent under reduced pressure the title compounds (**6-6u**) were isolated as amorphous solids after precipitation with hexane and/or diethyl ether. Confirmation of the structure of the thioamides was obtained by mass spectroscopy.

2-Cyano-3-imino-N-(4-trifluoromethyl-phenyl)thiobutyramide, 6. 3-Iminobutyronitrile (1.0 g, 12.2 mmol) and 4-trifluoromethyl-phenyl isothiocyanate (2.5 g, 12.2 mmol) were refluxed in dioxane (50 mL) for 3 h. After removal of the solvent, the crude was taken up with hexane and diethyl ether. The resulting amorphous solid was filtered off and dried to give **6** as a tautomeric mixture (3.1 g, 89%): ¹H NMR (DMSO-*d*₆) δ 9.3 (s, NH), 11.43 (s, NH₂), 7.7 (d, $J = 8.3$, 2H), 7.6 (d, $J = 8.3$, 2H), 2.3 (s, 3H). Anal. (C₁₂H₁₀F₃N₃S) C, H, N.

5-Methyl-3-(Rb)-1H-pyrazole-4-carbonitriles 3-3u: General Procedure. Thioamide **6-6u** (1 equiv) and hydrazine hydrate (1.2 equiv) were dissolved in EtOH (5 mmol of starting material in ~50 mL) and refluxed for 2-3 h. After removal of the solvent, the crude was treated with hexane and/or diethyl ether and then purified by chromatography. Elution with EtOAc afforded analytically pure **3-3u** (yields 70-85%). Melting points ($^{\circ}$ C) are as follows:

3a	3b	3c	3d	3e	3f	3g
261-265	156-157	214-215	210-211	231-234	224-226	>265
3h	3i	3j	3k	3l	3m	3n
232-236	240-244	207-210	225-228	217-219	213-217	217-220
3o	3p	3q	3r	3s	3t	3u
219-222	205-207	223-224	254-256	267-269	294-295	amorph

5-Methyl-3-(4-trifluoromethyl-phenyl)-1H-pyrazole-4-carbonitrile, 3. A solution of **6** (1.5 g, 5.7 mmol) and hydrazine hydrate (340 μ L, 6.8 mmol) in ethanol (50 mL) was refluxed for 2 h. After cooling at room temperature, the solvent was evaporated, and crude **3** was isolated after trituration with hexane. Chromatographic purification (eluent: EtOAc) gave pure **3** (1.0 g, 70%): mp 258-260 $^{\circ}$ C; ¹H NMR

(DMSO- d_6) δ 12.35 (s, NH), 9.23 (s, NH), 7.55 (m, 4H), 2.35 (s, 1H). Anal. (C₁₂H₉F₃N₄) C, H, N.

5-Amino-3-((4-trifluoromethyl-phenyl)amino)-1H-pyrazole-4-carbonitrile, 3v. An analogous procedure to that used for the synthesis of compound **8** in which malononitrile was used instead of ethyl cyanoacetate gave **3v** (0.29 g, 77%): mp 210–213 °C; ¹H NMR (DMSO- d_6) δ 11.35 (s, 1H, NH), 8.88 (s, 1H, NH), 7.60 (d, J = 8.3, 2H), δ 7.50 (d, J = 8.3, 2H), 6.35 (s, 2H, NH₂). Anal. (C₁₁H₈F₃N₅) C, H, N.

5-Ethylamino-3-((4-trifluoromethyl-phenyl)amino)-1H-pyrazole-4-carbonitrile, 3w. To a solution of **3v** (0.30 g, 1.23 mmol) and acetaldehyde (125 μ L, 2.25 mmol) in 20 mL of dioxane was added NaCNBH₃ (0.14 g, 2.25 mmol) under continuous stirring. After adjustment of the pH in the range of 4.6–5.0 (10% aqueous H₃PO₄), the reaction mixture was kept at room temperature for 90 min. Additional acetaldehyde (192 μ L, 3.37 mmol) and NaCNBH₃ (0.21 g, 3.37 mmol) was added and the reaction mixture was kept again at room temperature for a further 2 h. Dioxane was removed under reduced pressure, and the aqueous phase was extracted twice with EtOAc. The organic layer was dried over Na₂SO₄ and concentrated. Chromatographic purification of the crude (eluent: toluene/EtOAc, 1/1) afforded **3w** (0.12 g, 33%): mp 217–222 °C; ¹H NMR (DMSO- d_6) δ 11.63 (s, NH), 8.93 (s, NH), 7.64 (d, J = 8.3, 2H), δ 7.52 (d, J = 8.3, 2H), 6.94 (t, J = 6.2, 2H, NH₂), 3.15 (q, J = 6.2, 2H), 1.15 (t, J = 6.2, 3H). Anal. (C₁₃H₁₂F₃N₅) C, H, N.

2-Cyano-3-methylsulfanyl-3-((4-trifluoromethyl-phenyl)amino)acrylic Acid Ethyl Ester, 7. To a stirred solution of ethyl cyanoacetate (2.26 g, 20 mmol) in DMF (20 mL) was added NaH (0.8 g, 25 mmol) in portions under argon over a period of 30 min. The resulting yellow solution was further stirred for 30 min at room temperature, and 4-trifluoromethyl-phenyl isothiocyanate (4.8 g, 23.6 mmol) dissolved in DMF (2 mL) was added dropwise within 5 min. Subsequently, MeI (1.26 mL, 24.4 mmol) in DMF (3 mL) was added, and stirring was continued overnight. The reaction was quenched by carefully pouring it onto water (400 mL) and was extracted with EtOAc. The organic layer was dried over Na₂SO₄ and concentrated under reduced pressure to a semicrystalline residue which after two recrystallizations from a small amount of EtOH afforded **7** (4.0 g, 61%): mp 84–85 °C; ¹H NMR (DMSO- d_6) δ 11.9 (s, NH), 7.63 (m, 4H), 4.1 (q, J = 6.3, 2H), 2.32 (s, 3H), 1.17 (t, J = 6.3, 3H). Anal. (C₁₄H₁₃F₃N₂O₂S) C, H, N.

5-Hydroxy-3-((4-trifluoromethyl-phenyl)amino)-1H-pyrazole-4-carbonitrile, 4, and 5-Amino-3-((4-trifluoromethyl-phenyl)amino)-1H-pyrazole-4-carboxylic Acid Ethyl Ester, 8. A methanolic solution (40 mL) of **7** (0.46 g, 1.4 mmol) containing hydrazine hydrate (84 μ L, 1.7 mmol) was refluxed for 3 h. After cooling to room temperature, MeOH was removed under vacuum and the crude was chromatographed (eluent gradient: toluene/EtOAc, 1/1, \rightarrow EtOAc) to give **8** (0.33 g, 73%): mp 239–242 °C; ¹H NMR (DMSO- d_6) δ 11.24 (s, 1H, NH), 8.39 (s, 1H, NH), 7.75 (d, J = 8.3, 2H), 7.56 (d, J = 8.3, 2H), 6.14 (s, 2H), 4.22 (q, J = 6.3, 2H), 1.30 (t, J = 6.3, 3H). Anal. (C₁₃H₁₃F₃N₄O₂) C, H, N. **4** was also obtained (80 mg, 20%): amorphous; ¹H NMR (DMSO- d_6) δ 9.68 (s, 1H, NH), 8.33 (s, 1H, OH), 7.54 (d, J = 8.3, 2H), 7.42 (d, J = 8.3, 2H). Anal. (C₁₁H₇F₃N₄O) C, H, N.

2-Amino-6-oxocyclohex-1-enylthiocarbonyl-4-trifluoromethyl-phenylanilide, 9. To a stirred solution of 2-amino-cyclohexenone (3.0 g, 27.0 mmol) in CH₃CN (50 mL) was dropwise added (*p*-CF₃)PhNCS (27.6 mmol). The solution was refluxed overnight, cooled, and concentrated to one-half its volume. The resulting crystals were filtered and dried to afford **9** as a tautomeric mixture (3.96 g, 47%): mp 201–203 °C; ¹H NMR (DMSO- d_6) δ 14.91 (s, NH), 12.46 (s, NH₂), 9.31 (s, NH₂), 7.21 (s, 4H), 2.72 (t, J = 6.0, 2H), 2.47 (t, J = 6.0, 2H), 1.78 (m, 2H). Anal. (C₁₄H₁₃F₃N₂OS) C, H, N.

3-((4-Trifluoromethyl-phenyl)amino)-1,5,6,7-tetrahydroindazol-4-one, 10. To a solution of **9** (3.9 g, 12.6 mmol) in EtOH (100 mL) was added hydrazine hydrate (0.73 mL, 15.0 mmol). The solution was refluxed overnight and cooled to

room temperature, and the resulting precipitate was filtered and washed with diethyl ether to give **10** (2.4 g, 65%): mp 262–263 °C; ¹H NMR (DMSO- d_6) δ 12.62 (s, NH), 8.40 (s, NH), 7.80 (d, J = 7.8, 2H), 7.57 (t, J = 7.8, 2H), 2.82 (d, J = 6.0, 2H), 2.49 (t, J = 6.2, 2H), 2.05 (dd, J = 6.0, J = 6.2, 2H). Anal. (C₁₄H₁₂F₃N₃O) C, H, N.

(4,5,6,7-Tetrahydro-1H-indazol-3-yl)(4-trifluoromethyl-phenyl)amine, 11. To a cooled (–78 °C) suspension of LiAlH₄ (0.39 g, 7.5 mmol) in dry THF (50 mL) was added a solution of concentrated H₂SO₄ (0.27 mL) in THF (2.7 mL) dropwise, and the reaction was allowed to reach room temperature. After addition of the ketone **10** (0.74 g, 2.5 mmol) in THF (7.4 mL) and further stirring for 15 min, the reaction was quenched with a saturated solution of Na₂SO₄ (1.1 mL). Evaporation to dryness and purification of the crude by chromatography (eluent: hexane/EtOAc, 2/1) afforded **11** (0.5 g, 60%): mp 161–163 °C; ¹H NMR (DMSO- d_6) δ 11.71 (s, NH), 8.37 (s, NH), 7.42 (s, 4H), 2.52 (t, J = 6.1, 2H), 2.31 (t, J = 6.1, 2H), 1.69 (m, 4H). Anal. (C₁₄H₁₄F₃N₃) C, H, N.

3-Oxo-2-phenyl-N-(4-trifluoromethyl-phenyl)thiobutamide, 12. To a solution of (4-CF₃)PhNCS (2.0 g, 9.7 mmol) in dry THF (10 mL) was added NaH (0.58 g, 14.5 mmol). To the cooled (0 °C) mixture was dropwise added a solution of benzyl methyl ketone (1.95 mL, 14.5 mmol) in THF (10 mL) at such a rate that the temperature did not exceed 40 °C. The reaction was further stirred for 12 h at room temperature and then allowed to rest. To the crystalline mass formed was added water (100 mL) carefully, and the resulting solution was extracted with diethyl ether. The organic phase was discarded and the aqueous one acidified to pH 5 with 2 N HCl. To the oily layer which separated was added CH₂Cl₂ (15 mL), and the solution was dried over Na₂SO₄ and concentrated in a vacuum to give **12** as a red oil (3.05 g, 93%) which was used in the next step without further purification: ¹H NMR (DMSO- d_6) δ 11.22 (s, NH), 7.47 (m, 9H), 5.51 (s, 1H), 2.34 (s, 3H).

2-(1-Iminoethyl)-3-oxo-N-(4-trifluoromethyl-phenyl)thiobutamide, 13. 4-Aminopent-3-en-2-one (0.50 g, 5.0 mmol) and (4-CF₃)PhNCS (0.84 g, 5.5 mmol) were dissolved in dry dioxane (5 mL), and the solution was refluxed for 4 h. After evaporation of the solvent to dryness and addition of a small amount of CH₂Cl₂, the crude crystallized. The crystals were collected and thoroughly washed with CH₂Cl₂ to give **13** (0.74 g, 48%): mp 168–170 °C; ¹H NMR (DMSO- d_6) δ 12.00 (s, NH), 10.19 (s, NH), 8.19 (d, J = 7.8, 2H), 7.82 (br s, OH), 7.78 (d, J = 7.8, 2H), 2.32 (s, 3H), 2.383 (s, 3H). Anal. (C₁₃H₁₃F₃N₃OS) C, H, N.

(5-Methyl-4-phenyl-1H-pyrazol-3-yl)(4-trifluoromethyl-phenyl)amine, 14. A solution of **12** (2.0 g, 9.6 mmol) in EtOH (30 mL) containing hydrazine hydrate (0.34 mL, 7.1 mmol) was refluxed overnight and then allowed to reach room temperature. Upon concentration of the solvent to approximately 5 mL, crystallization occurred. The solid was filtered and dried to afford **14** (0.28 g, 15%): mp 139–145 °C; ¹H NMR (DMSO- d_6) δ 12.32 (s, NH), 8.17 (s, NH), 7.30 (m, 9H), 2.39 (s, 3H). Anal. (C₁₇H₁₄F₃N₃) C, H, N.

[4-(1-Hydrazonoethyl)-5-methyl-1H-pyrazol-3-yl](4-trifluoromethyl-phenyl)amine, 15, and 3-((4-Trifluoromethyl-phenyl)amino)-1H-pyrazole-4-carbonitrile, 16. A solution of **13** (0.31 g, 1.0 mmol) in EtOH (12 mL) containing hydrazine hydrate (0.24 mL, 4.9 mmol) was refluxed for 2 h and allowed to cool to room temperature. After removal of the solvent and chromatography of the crude (eluent: hexane/EtOAc, 1/3) pyrazole **16** was isolated (82 mg, 29%): mp 151–153; ¹H NMR (DMSO- d_6) δ 11.35 (s, NH), 9.58 (s, NH), 7.55 (m, 5H), 2.30 (s, 1H). Anal. (C₁₁H₁₀F₃N₄) C, H, N. Hydrazone **15** was isolated as well (85 mg, 29%): mp 196–198 °C; ¹H NMR (DMSO- d_6) δ 12.62 (s, NH), 11.45 (s, NH), 8.05 (d, J = 7.8, 2H), 7.75 (d, J = 7.8, 2H), 2.08 (s, 3H), 1.97 (s, 3H). Anal. (C₁₃H₁₄F₃N₅) C, H, N.

5-Methyl-3-((4-trifluoromethyl-phenyl)amino)-1H-pyrazole-4-carboxylic Acid Ethyl Ester, 17. To a suspension of *p*-trifluoromethyl-phenylthiosemicarbazide (3.4 g, 14.4 mmol) in dry EtOH (40 mL) was slowly added concentrated HCl (4.3 mL) at room temperature. After the mixture stirred for 10

min, a solution of ethyl 2-chloroacetate (2.12 mL, 14.5 mmol) in EtOH (10 mL) was added dropwise resulting in a gradual dissolution of the suspension. Further refluxing for 4 h resulted in the formation of elemental sulfur which was removed by filtration. The filtrate was concentrated in a vacuum, and the solid obtained was recrystallized from EtOH to yield **17** (2.8 g, 62%): mp 214–217 °C; ¹H NMR (DMSO-*d*₆) δ 12.5 (s, NH), 8.55 (s, NH), 7.74 (d, *J* = 7.8, 2H), 7.58 (d, *J* = 7.8, 2H), 4.23 (q, *J* = 6.4, 2H), 2.42 (s, 3H), 1.32 (t, *J* = 6.4, 3H). Anal. (C₁₄H₁₄F₃N₃O₂) C, H, N.

[5-Methyl-3-(4-trifluoromethyl-phenyl)amino]-1H-pyrazol-4-yl]methanol, 18. A solution of H₂SO₄ (0.17 mL, 3.2 mmol) in dry THF (1.7 mL) was dropwise added to a suspension of LiAlH₄ (0.25 g, 6.4 mmol) in THF at –78 °C. The resulting solution was allowed to reach room temperature and was further stirred for 15 min. A solution of the ester **17** (0.5 g, 1.6 mmol) in THF (2.0 mL) was slowly added, and the reaction was stirred until no more ester was present (approximately 15 min) as judged by TLC analysis. The reaction was then quenched first by the careful addition of saturated aqueous Na₂SO₄ (1.1 mL) and 10 min later by a 30% aqueous solution of NaOH (0.5 mL). Diethyl ether was added, and the resulting precipitate was removed by filtration. The filtrate was dried (MgSO₄), evaporated to dryness, and chromatographed (eluent: hexane/EtOAc, 1/2) to give **18** (0.50 g, 12%): mp 187–190 °C; ¹H NMR (DMSO-*d*₆) δ 11.87 (s, NH), 8.18 (s, NH), 7.47 (m, 4H), 4.52 (t, *J* = 6.0, OH), 4.31 (d, *J* = 6, 2H), 2.19 (s, 3H). Anal. (C₁₂H₁₂F₃N₃O) C, H, N.

(4,5-Dimethyl-1H-pyrazol-3-yl)(4-trifluoromethyl-phenyl)amine, 19. A solution of **17** (0.82 g, 2.6 mmol) in THF was dropwise added to a refluxing suspension of LiAlH₄ (0.5 g, 12.8 mmol) in dry THF (20 mL). After further refluxing for 2 h, TLC analysis showed the absence of starting material. The reaction was allowed to cool to room temperature and was carefully quenched first with a slow addition of EtOH (5 mL) and then with an aqueous saturated solution of Na₂SO₄. Extraction with EtOAc followed by chromatography of the crude (eluent: hexane/EtOAc, 1/2) afforded dimethylpyrazole **19** (80 mg, 11%): mp 129–132 °C; ¹H NMR (DMSO-*d*₆) δ 7.43 (d, *J* = 7.8, 2H), 7.02 (d, *J* = 7.8, 2H), 6.12 (s, NH), 2.23 (s, 3H), 1.85 (s, 3H). Anal. (C₁₂H₁₂F₃N₃) C, H, N.

5-Methyl-3-[methyl(4-trifluoromethyl-phenyl)amino]-1H-pyrazole-4-carbonitrile, 20. To a cooled (–78 °C) solution of **3** (0.50 g, 1.9 mmol) in dry THF (60 mL) was dropwise added BuLi (3.6 mL of a 1.6 M solution in hexane, 5.7 mmol). After the mixture stirred at this temperature for 30 min, MeI (0.35 mL, 5.7 mmol) was added and the reaction was allowed to reach room temperature and quenched with water. Extraction with EtOAc followed by chromatography of the crude (eluent: EtOAc/hexane, 2/1) gave **20** (17 mg, 34%): mp 146–147 °C; ¹H NMR (DMSO-*d*₆) δ 7.55 (d, *J* = 7.2, 2H), 7.03 (d, *J* = 7.2, 2H), 3.37 (s, 3H), 2.32 (s, 3H).

1,3-Dimethyl-5-(4-trifluoromethyl-phenyl)amino)-1H-pyrazole-4-carbonitrile, 21. Same procedure as for compound **3**, but instead of hydrazine hydrate as reagent *N*-methylhydrazine was used (0.90 g, 56%): amorphous; ¹H NMR (DMSO-*d*₆) δ 9.15 (s, NH), 7.58 (d, *J* = 8.3, 2H), 6.93 (d, *J* = 8.3, 2H), 3.62 (s, 3H). Anal. (C₁₃H₁₁F₃N₄) C, H, N.

(2) Biology. Inhibition of T-Cell-Independent B-Cell Antigen Responses to TNP-LPS. Culturing of Spleen Cells To Elicit In Vitro Antibody Responses. Spleens from C57Bl/6 nu/nu and C57Bl/6 mice were cultured in duplicate in flat bottomed microtiter plates (2 × 10⁵ cells/well). Serial dilutions of drug solutions in serum-supplemented culture medium (IMDM-ATL + 10% FCS)³⁴ were added to a final volume of 0.2 mL in the presence of optimal concentration of TNP-LPS. The stimulated spleen cells were cultured for 4 days at 37 °C in a humidified CO₂ incubator (5.5%), and then the antigen supernatant from each of the two replicate cultures were pooled and diluted 4-fold in PBS/BSA or PBS/HSA and assayed in an ELISA.

ELISA Quantification. The readout used to determine antibodies induced by TNP-LPS was based on the high cross-reactivity of antibodies against DNP (dinitrophenol) and TNP

(trinitrophenol). ELISA plates were coated with BSA-DNP by overnight incubation at 4 °C, and after removal of BSA-DNP solution residual protein-binding sites were blocked with 2% BSA or 5% human albumin in PBS. Plates were washed three times with PBS containing 0.05% Tween 20 and 0.02% Na₂S₂O₃ between each step. Serial dilutions of the supernatants in 2% BSA-PBS were incubated overnight at 4 °C. Bound IgM Abs was revealed using biotin-labeled affinity-purified goat anti-mouse IgM antibody (1:15000; 2 h at 37 °C) and, subsequently, streptavidin conjugated to alkaline phosphatase (1:10000 for 1 h at 37 °C). Enzyme activity was determined after addition of *p*-nitrophenyl phosphate (1 mg/mL) in 1 M diethanolamine, pH 9.8, by measuring the absorbency at 405/490 nm with a Spectra Max reader usually after 30–45 min of incubation at room temperature. Absorbance values obtained in the absence of stimulus were used as low control; absorbency values obtained in the presence of the stimulus were taken as high control. Percent inhibition of the signal by the samples was calculated according to the equation: inhibition(%) = [(high – low) – (sample – low)] / (high – low) × 100.

Mouse Mixed Lymphocyte Reaction (MLR-M).³¹ Equal amounts of spleen cells from C57/Bl6 mice (H-2^b) and CBA/2 mice (H-2^k) were mixed; 4 × 10⁵ cells/well were incubated with appropriate serial dilutions (DMSO/water) of drug samples in 200 μL of complete RPMI medium in flat bottom tissue culture microtiter plates for 4 days at 37 °C in 5% CO₂. Proliferation was assessed by [³H]thymidine incorporation.

Proliferation of the Human T-Cell Line Jurkat. The cell line was maintained and propagated in fetal calf serum-supplemented RPMI medium; 5 × 10⁴ cells/well were incubated in 200 μL of RPMI medium for 2 days. [³H]Thymidine was measured at the end of the culture period.

(3) Pharmacokinetics. Male mice (OF1, ~25 g) either were administered a solution (ethanol + water + olive oil) of 0.612 mg of [³H]-**3** together with 69.4 mg of unlabeled **3** orally or were injected in the femoral vein with a solution (EtOH + poly(ethylene glycol) + 5% glucose) of 1.08 mg of [³H]-**3** together with 10.92 mg of nonlabeled **3**. Blood was collected from the vena cava (3 mice/time at 0.08, 0.5, 1, 2, 4, 8, 24 h after intravenous bolus and at 0.5, 1, 2, 4, 8, 24 h after oral administration). All collected samples were assayed for total radioactivity by LSC and for parent compound by LC–RID.

An analogous protocol was applied for the assessment of the plasma concentration of **3o** as function of time. Electrospray mass spectroscopy was used for the detection of the parent compound, and quantitation was based on integration of the peaks corresponding to the ion *m/z* 156.

Acknowledgment. We express our warmest thanks to Dr. H. Andres for the labeling of **3** and Ms. Corinne Simeon and Mr. Armin Brülisauer, Hellmut Knecht, Xaver Borer, and Andrea Florineth for their skillfull technical assistance.

Supporting Information Available: Detailed crystallographic data concerning the two forms of **3** (8 pages). Ordering information is given on any current masthead page.

References

- Perico, N.; Remuzi, G. Prevention of transplant rejection. Current treatment guidelines and future developments. *Drugs* **1997**, *54*, 533–570.
- Braendle, D.; Joergensen, J.; Zenke, G.; Buerki, K.; Hof, R. P. Evidence from B Cell-Deficient Mice treated with Cyclosporin A that Donor-Specific Antibodies contribute to Acute Allograft Rejection. *Transplantation* **1998**, in press.
- Platt, J. L. Xenotransplantation. *Sci. Med.* **1996**, *2*, 62–71. Lawson, J. H.; Platt, J. L. Molecular barriers to xenotransplantation. *Transplantation* **1996**, *62*, 303–310. Saadi, S.; Platt, J. L. Immunology of xenotransplantation. *Life Sci.* **1998**, *62*, 365–387.
- Dorling, A. Strategies for preventing porcine xenograft rejection: recent progress and future developments. *Exp. Opin. Ther. Patents* **1997**, *7*, 1307–1319.

- (5) Dalamso, A. P.; Bach, F. H. Expression of human regulators of complement on pig endothelial cells. *Xenotransplantation* **1996**, *4*, 55–57. Cozzi, E.; White, D. J. G. The generation of transgenic pigs as potential organ donors for humans. *Nature Med.* **1995**, *1*, 964–966.
- (6) Lin, Y.; Goebels, J.; Xia, G.; Ji, P.; Vandeputte, M.; Waer, M. Induction of specific transplantation tolerance across xenogeneic barriers in the T-independent immune compartment. *Nature Med.* **1998**, *4*, 173–180.
- (7) Lawson, J. H.; Daniels, L. J.; Hoopes, C. W.; Lin, S. S.; Weidner, B. C.; Mccurry, K. R.; Davis, R. D.; Bollinger, R. R.; Harland, R. C.; Logan, J.; Diamond, L. E.; Martin, M.; Byrne, G.; Platt, J. L. The role of transgenic expression of human complement regulatory proteins in discordant xenotransplantation. *Surg. Forum* **1997**, *48*, 487–489 Leventhal, J. R.; Sakiyalak, P.; Witson, J.; Simone, P.; Matas, A. J.; Bolman, R. M.; Dalmasso, A. P. The synergistic effect of combined antibody and complement depletion on discordant cardiac xenograft survival in non-human primates. *Transplantation* **1994**, *57*, 974–977. Leventhal, J. R.; Matas, A. J.; Sun, L. H.; Reif, S.; Bolman, R. M.; Dalmasso, A. P.; Platt, J. L. The immunopathology of cardiac xenograft rejection in the guinea pig-to-rat model. *Transplantation* **1993**, *56*, 1–8. Blakely, M. L.; van der Werf, W. J.; Berndt, M. C.; Dalmasso, A. P.; Bach, F. H.; Hancock, W. W. Activation of intragraft endothelial and mononuclear cells during discordant xenograft rejection. *Transplantation* **1994**, *58*, 1059–1066. Soheyla, S.; Platt, J. L. Immunology of xenotransplantation. *Life Sci.* **1997**, *62*, 365–387.
- (8) Häry, P. Molecular Pathology of Acute and Chronic Rejection. *Transplant. Proc.* **1994**, *26*, 3280–3284. Azuma, H.; Tilney, N. L. Chronic graft rejection. *Curr. Opin. Immunol.* **1994**, *6*, 770–776.
- (9) Hess, M. L.; Hastillo, A.; Mohanakumar, D. V. M.; Cowley, M. J.; Vetrovac, G.; Szentpetery, S.; Wolfgang, T. C.; Lower, R. R. Accelerated atherosclerosis in cardiac transplantation: role of cytotoxic B-cell antibodies and hyperlipidemia. *Circulation* **1983**, *68* (Suppl. II), II-94, II-101. Diethelm, A. G.; Deierhoi, M. H.; Hudson, S. L.; Laskow, D. A.; Julian, B. A.; Gaston, R. S.; Bynon, J. S.; Cutris, J. J. Progress in renal transplantation. A single center study of 3359 patients over 25 years. *Ann. Surg.* **1995**, *221*, 446–457. Lobo, P. I.; Spencer, C. E.; Stevenson, W. C.; Pruett, T. L. Evidence demonstrating poor kidney graft survival when acute rejections are associated with IgG donor-specific lymphocytotoxin. *Transplantation* **1995**, *59*, 357–360. Suciu-Foca, N.; Reed, E.; Marboe, C.; Harris, P.; Xi, Y. P.; Yu-Kai, S.; Ho, E.; Rose, E.; Reemtsma, K.; King, D. W. The role of Anti-HLA Antibodies in Heart Transplantation. *Transplantation* **1991**, *57*, 716–724. Winter, J. B.; Clelland, C.; Gouw, A. S.; Prop, J. Distinct phenotypes of infiltrating cells during acute and chronic lung rejection in human heart-lung transplants. *Transplantation* **1995**, *59*, 63–69.
- (10) Shi, C.; Lee, W.-S.; He, Q.; Zhang, D.; Fletcher, D. L.; Newell, J. B.; Haber, E. Immunological basis of transplant-associated arteriosclerosis. *Proc. Natl. Acad. Sci. U.S.A.* **1996**, *93*, 4051–4056.
- (11) Silva, H. T.; Morris, R. E. Leflunomide and malononitriloamides. *Exp. Opin. Invest. Drugs* **1997**, *6*, 51–64.
- (12) Lucien, J.; Marath, A.; Rayat, G.; Koshal, A.; Yatscoff, R. Efficacy of Leflunomide to Reduce Xenobody Titers In Vivo: An Evaluation of the Prolongation of Discordant Xenograft Survival. *Transplant. Proc.* **1996**, *28*, 704–707. Lin, Y.; Sobis, H.; Vandeputte, M.; Waer, M. Long-Term Xenograft Survival and Suppression of Xenobody Formation in the Hamster-to-Rat Heart Transplant Model Using a Combination Therapy of Leflunomide and Cyclosporin. *Transplant. Proc.* **1994**, *26*, 3202. Xiao, F.; Chong, A.; Foster, P.; Sankary, H.; McChesney, L.; Koukoulis, G.; Yang, J.; Frieders, D.; Williams, J. W. Leflunomide Controls Rejection in Hamster to Rat Cardiac Xenografts. *Transplantation* **1994**, *58*, 828–834. Lin, Y.; Sobis, H.; Vandeputte, M.; Waer, M. Mechanism of Leflunomide-Induced Prevention of Xenobody Formation and Xenograft Rejection in the Hamster to Rat Heart Transplantation Model. *Transplant. Proc.* **1995**, *27*, 305–306.
- (13) MacDonald, A. S.; Sabr, K.; MacAuley, M. A.; McAlister, V. C.; Bitter-Suermann, H.; Lee, T. Effects of Leflunomide and Cyclosporin on Aortic Allograft Chronic Rejection in the Rat. *Transplant. Proc.* **1994**, *26*, 3244–3245. Morris, R. E.; Huang, X.; Gregory, C. R.; Billingham, M. E.; Rowan, R.; Shorthouse, R.; Berry, G. J. Studies in Experimental Models of Chronic Rejection: Use of Rapamycin and Isoxazole Derivatives for the Suppression of Graft Vascular Disease and Obliterative Bronchiolitis. *Transplant. Proc.* **1995**, *27*, 2068–2069. Swan, S. K.; Grary, G. S.; Guijarro, C.; O'Donnell, M. P.; Keane, W. F.; Kasiske, B. L. Immunosuppressive Effects of leflunomide in Experimental Chronic Vascular Rejection. *Transplantation* **1995**, *60*, 887–890. Xiao, F.; Chong, A.; Shen, J.; Yang, J.; Short, J.; Foster, P.; Sankary, H.; Jensik, S.; Mital, D.; McChesney, L.; Koukoulis, G.; Williams, J. W. Pharmacologically Induced Regression of Chronic Transplant Rejection. *Transplantation* **1995**, *60*, 1065–1072.
- (14) Dias, V. C.; Lucien, J.; LeGatt, D. F.; Yatscoff, R. W. Measurement of the Active Leflunomide Metabolite by Reverse-Phase High-Performance Liquid Chromatography. *Ther. Drug Monitor.* **1995**, *17*, 84–88.
- (15) Kuo, E. A.; Hambleton, P. T.; Kay, D. P.; Evans, P. L.; Matharu, S. S.; Little, E.; McDowall, N.; Jones, B. C.; Hedgecock, C. J. R.; Yea, C. M.; Chan, E. A. W.; Hairsine, P. W.; Ager, I. A.; Tully, R. W.; Williamson, R. A.; Westwood, R. *J. Med. Chem.* **1996**, *39*, 4608–4612.
- (16) Shuurman, H.-J.; Tanner, M. Unpublished results (NOVARTIS Pharma AG).
- (17) Papageorgiou, C.; Zurini, M.; Weber, H.-P.; Borer, X. Leflunomide's Bioactive Metabolite Has the Minimal Structural Requirements for the Efficient Inhibition of Human Dihydroorotate Dehydrogenase. *Bioorg. Chem.* **1997**, *25*, 233–238.
- (18) Papageorgiou, C.; Kayan, A.; Oberer, L.; Borer, X.; Rihs, G. Hydroxy- and Alkoxy-Cyanopropenamides: Synthesis, Structure and Solvent Dependent (E)/(Z) Isomerisation. *Helv. Chim. Acta* **1998**, *81*, 1319–1328.
- (19) Bertolini, G.; Aquino, M.; Biffi, M.; d'Atri, G.; Di Pierro, F.; Ferrario, F.; Mascagni, P.; Somenzi, F.; Zaliani, A.; Leoni, F. A New Rational Hypothesis for the Pharmacophore of the active Metabolite of Leflunomide, a Potent Immunosuppressive Drug. *J. Med. Chem.* **1997**, *40*, 2011–2016.
- (20) Ibrahim, N. S. Reaction of isothiocyanates with active methylene reagent: a new approach for the synthesis of pyrazole, pyrimidine and pyrazolo[1,5-a]pyrimidine derivatives. *Chem. Ind.* **1989**, 654–655.
- (21) Mohareb, R. M.; Shams, H. Z.; Aziz, S. I. Reactions with 4-Phenyl-3-thiosemicarbazide: A New Approach for the Synthesis of Pyrazole, Thiazole, Pyridine and Pyrazolo[3,4-b]pyridine derivatives. *Sulfur Lett.* **1991**, *13*, 101–113.
- (22) Vishwakarma, J. N.; Chowdhury, B. K.; Roy, H.; Jumjappa, H. Reactions of polarized ketene S,N-acetals with hydrazine: a facile general route to 3(5)-substituted amino-4,5(3)-substituted pyrazoles. Part XLV. *Indian J. Chem., Sect. B* **1985**, *24B*, 472–476.
- (23) Hackler, R. E.; Wickiser, D. I. 3-Substituted 3-aminonitriles. Patent GB 2141712 A, Jan 3, 1985.
- (24) Lang, S. A.; Cohen, E. β -Aminocinnamionitriles as potent anti-inflammatory agents. *J. Med. Chem.* **1975**, *18*, 441–443.
- (25) Suesse, M.; John, S. Synthese von Chinazolin-4-thion- und 1H-Indazol-Derivaten. (Synthesis of Quinazoline-4-thiones and 1H-Indazole Derivatives.) *J. Prakt. Chem.* **1986**, *328*, 635–639.
- (26) Goerdeler, J.; Laqua, A.; Linder, C. Imidoylketene imines. II. Preparation of vinylogous thioureas and isothioureas. *Chem. Ber.* **1974**, *107*, 3518–3532.
- (27) Radl, S. Preparation of some pyrazole derivatives by extrusion of elemental sulfur from 1,3,4-thiadiazines. *Collect. Czech. Chem. Commun.* **1992**, *5*, 656–659.
- (28) Taylor, R.; Kennard, O. Crystallographic Evidence for Existence of C-H \cdots O, C-H \cdots N, and C-H \cdots Cl Hydrogen Bonds. *J. Am. Chem. Soc.* **1982**, *104*, 5063–5070.
- (29) The molecular modeling program packet Sybyl6.4 r4, from Evans & Sutherland, Tripos Assoc. Inc., St. Louis, MO, was used.
- (30) Kallen, J.; Mikol, V.; Quesniaux, V.; Walkinshaw, M. D.; Schneider-Scherzer, E.; Schorgendorfer, K.; Weber, G.; Fliri, H. G. Cyclosporins: recent developments in biosynthesis, pharmacology and biology, and clinical applications. In *Biotechnology*, 2nd ed.; Kleinkauf, H., Von Doehren, H., Eds.; VCH: Weinheim, Germany, 1997; pp 535–591.
- (31) Meo, T. The MLR test in the mouse. In *Immunological Methods*; Lefkovits, I., Pernis, B., Eds.; Academic Press: New York, 1979; pp 227–239.
- (32) Davies, J. P.; Cain, G. A.; Pitts, W. J.; Magolda, R. L.; Copeland, R. A. *Biochemistry* **1996**, *35*, 1270–1273.
- (33) Fersht, A. R. The hydrogen bond in molecular recognition. *Trends Biol. Sci.* **1987**, *13*, 301–304.
- (34) Schreier, M. H.; Tees, R. Long-term culture and cloning of specific helper T cells. In *Immunological Methods*; Lefkovits, I., Pernis, B., Eds.; Academic Press: New York, 1981; pp 263–275.

JM981028C